Proceedings of the ASME 2017 Turbo Expo
GT2017
June 26-30, 2017, Charlotte, USA

GT2017-63020

IMPACT OF WAKE DISPERSION ON AXIAL COMPRESSOR PERFORMANCE

Chunill Hah
NASA Glenn Research Center,
MS 5-10, Cleveland, Ohio

ABSTRACT

Rotor wake dispersion in a low-speed, one and half stage axial compressor is investigated in detail with a Large Eddy Simulation (LES). The primary focus is to quantify the total pressure recovery due to wake stretching and the total pressure loss from the rotor wake interaction with the stator blade boundary layer. The relative magnitude of the aerodynamic loss due to these two effects is examined at several radial locations. The spacing between the rotor and the stator was varied from 29% to 112% of the rotor axial chord at the mid span to investigate the effects of rotor wake decay before entering the stator passage. The current analysis indicates that the efficiency through the compressor stage is increased about 0.5% when the spacing between the rotor and the stator is decreased from 112% to 29% of the rotor axial chord at mid-span. 22% of the efficiency gain from the narrower axial gap is due to the wake recovery and 63% is due to the stronger unsteady pressure field at the exit of the rotor due to stage interaction. Total pressure loss/recovery across the stator varies significantly in the radial direction for the current compressor, which has a much lower aspect ratio. The total pressure recovery due to wake stretching is larger than the total pressure loss due to the unsteady boundary layer development on the stator blade from 20% to 35% of the span from the hub for 29% spacing and from 35% to 55% of the span for 112% spacing. Above 50% of the span, rotor tip clearance flow affects wake dispersion and the overall wake recovery is less than expected.

INTRODUCTION

To improve the efficiency of large gas turbine engines, advanced high pressure ratio core compressors with fewer stages have been designed and tested recently. These core compressors are designed with current state-of-the-art design technology based on various types of Reynolds-averaged Navier-Stokes (RANS) codes and/or full unsteady Reynolds-averaged Navier-Stokes (URANS) code. Both pre- and post-test analysis suggest that the current generation of analysis tools based on RANS/URANS overestimate compressor performance significantly (for example, see Lurie and Breeze-Stringfellow [2015]). It is believed that some of the important flow physics inside such a highly-loaded compressor stage are not modeled, even with current state-of-the-art tools based on RANS and URANS. Consequently, details of the loss generation process are not yet fully understood and a three-dimensional picture of the loss generation in multi-stage compressors cannot be accurately predicted yet. Experimental investigation of the detailed loss generation process in multi-stage compressors is very expensive and the uncertainty of the obtained data is often larger than desired. Analytical tools that can provide

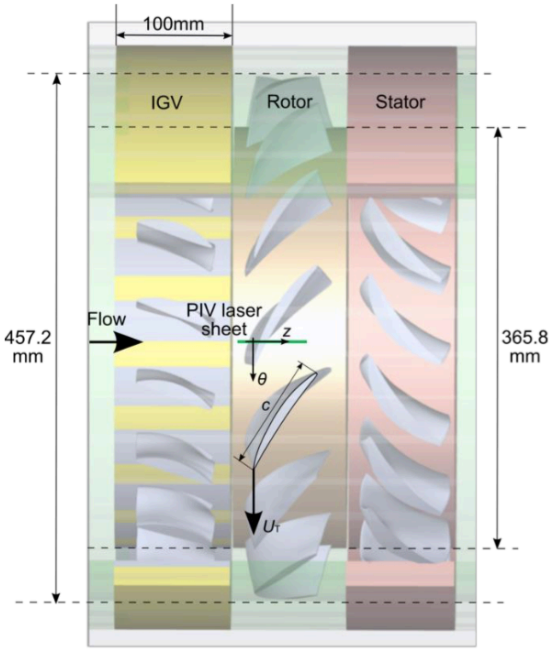

Figure 1. One and a half stage axial compressor

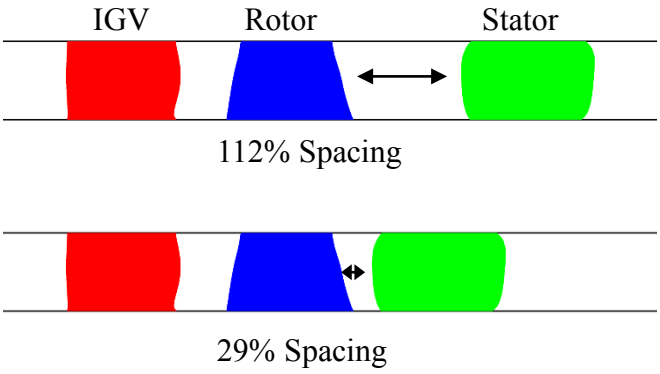

Figure 2. Cross section of two compressor configurations

accurate flow/loss development in multi-stage compressors are highly desirable. Therefore, it is necessary to develop and validate higher fidelity analysis tools capable of describing precisely how aerodynamic loss is generated and propagated in a multi-stage compressor.

Two important flow phenomena in multi-stage axial compressors are wake dispersion and upstream pressure propagation. Smith [1966, 1970] gave a very important physical description of wake dispersion in multi-stage axial compressors in his classical papers. He explained that wake stretching in the downstream blade rows gives total pressure recovery, and compressor performance is improved by the wake recovery. Van Zante et al. [2002] examined this wake recovery effect in a high-speed axial compressor. Their study indicates that the rotor wake stretching is the primary decay process in the stator passage. Adamczyk [1996] proposed that the wake recovery process is related to wake vorticity field kinematics and can be estimated using linear theory. Deregel and Tan [1996] used a 2-D time-accurate Navier-Stokes simulation to study rotor wake recovery. Valkov [1997] used a time-accurate Reynolds-averaged Navier-Stokes code to quantify the steady performance effect of an unsteady wake in a low-speed compressor stator. He also found that wake stretching is the dominant mechanism in the stator passage. Kerrebrock and Mikolajczak [1970] showed that the rotor wake, which has higher total pressure and higher total temperature in absolute frame than fluid in the free stream, is transported to the pressure side of the stator due to the slip velocity in the stator frame. Pallot et al. [2016] applied RANS and URANS to study the rotor wake attenuation in the stator passage in a low-speed single-stage compressor. Little experimental data about wake dispersion in multi-stage environments exist (for example, Ding [1982], Dunker [1983], Williams [1988], and Hathaway [1986]). These experimental studies provide the overall effect of wake dispersion on the steady performance of the compressor stage. To have a better understanding of the related flow physics and to advance multi-stage compressor design, detailed unsteady flow mechanisms inside the stator blade passage need to be understood quantitatively.

Stretching of the rotor wake in the stator passage is caused by inviscid effects. However, total pressure recovery due to the wake stretching is a viscous process where turbulent kinetic energy is converted to the mean energy, or negative generation of the turbulent kinetic energy. This negative generation process of the turbulent kinetic energy is not modeled in the frame of conventional RANS and URANS approaches. To obtain more

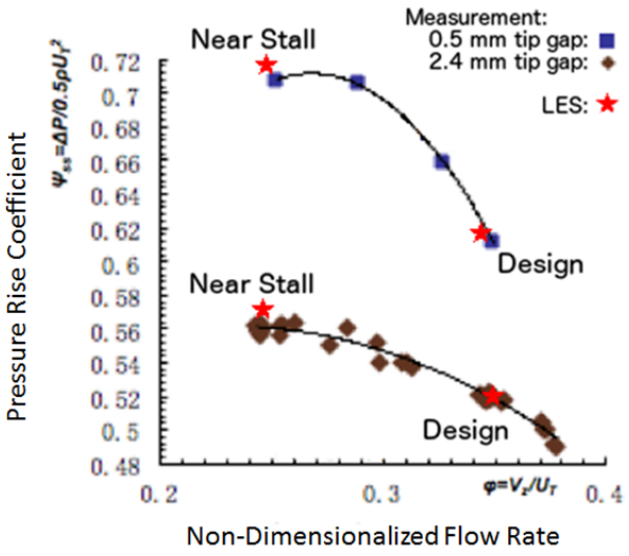

Figure 3. Pressure rise characteristics of the original compressor stage

realistic flow simulations, higher fidelity analysis tools based on Direct Numerical simulation (DNS) and LES are being applied for turbomachinery flow analysis (Zaki et al. [2010], Hah and Shin [2012], Gourdain [2013], Hah and Katz [2014], and Papadogiannis et al. [2014]).

The current paper is aimed to investigate rotor wake dispersion in the stator passage in detail. Total pressure recovery due to the wake stretching and total pressure loss due the interaction of the rotor wake with the stator blade are studied in detail with a fine-grid based LES. Spacing between the rotor and the stator was varied from 29% to 112% of the rotor axial chord at mid-span to quantify the effects of the unsteady rotor wake on the steady performance. The calculated flow fields from LES are compared with related measurements and examined in detail for the effects of wake dispersion at several radial locations.

ONE AND ONE HALF STAGE AXIAL COMPRESSOR AND LES SETUP

Figure 1 shows the one and one half stage axial compressor test rig configuration at Johns Hopkins University (JHU). For the current numerical investigation of wake dispersion, two congfigurations with different spacing between the rotor and the stator were selected. Cross sections of the two compressor configurations are shown in Figure 2. The JHU compressor, which is focused on investigating the flow physics of the rotor tip clearance flow field, is an aerodynamically scaled derivative of the first one and one half stages (i.e., inlet guide vane, rotor, and stator) of the NASA Glenn Research Center's Low-Speed Axial Compressor (LSAC), which comprises an IGV followed by four geometrically identical stages designed for an accurate low-speed simulation of a high-speed multi-stage core compressor (Wasserbauer, 1995). In addition, commensurate with the NASA LSAC compressor, the JHU compressor has a long entrance length to develop thick end wall boundary layers typical of an embedded stage. The target Reynolds number is 4.0×10^5 based on the tip speed and the rotor chord length at the tip. Details of the JHU compressor design parameters are given by Hah et al. [2014]. Extensive PIV measurements and a corresponding LES study have been conducted with two rotor tip clearances (0.8% and 4% of the rotor span). All previous experimental studies were conducted with an axial gap of 71% of the rotor axial chord at mid-span between the rotor and the stator. The compressor static pressure rise characteristic curves for two tip gaps with the original axial spacing from measurement and LES are given in Figure 3. A detailed comparison of the measured flow field from PIV and calculated flow field from the LES show that the LES captures the measured unsteady flow field inside this compressor remarkably well (for example, Hah [2016]). As the LES captures both steady and unsteady flow characteristics very well at the current compressor operating conditions, the LES is applied to study wake dispersion (mixing and stretching) at the design mass flow rate in Figure 3.

LES AND COMPUTATIONAL GRID

Effects of rotor wake dispersion/recovery in multi-stage compressors have been known for over 50 years since Smith [1966] explained the phenomena. However, no three-dimensional simulations explaining the effects of wake

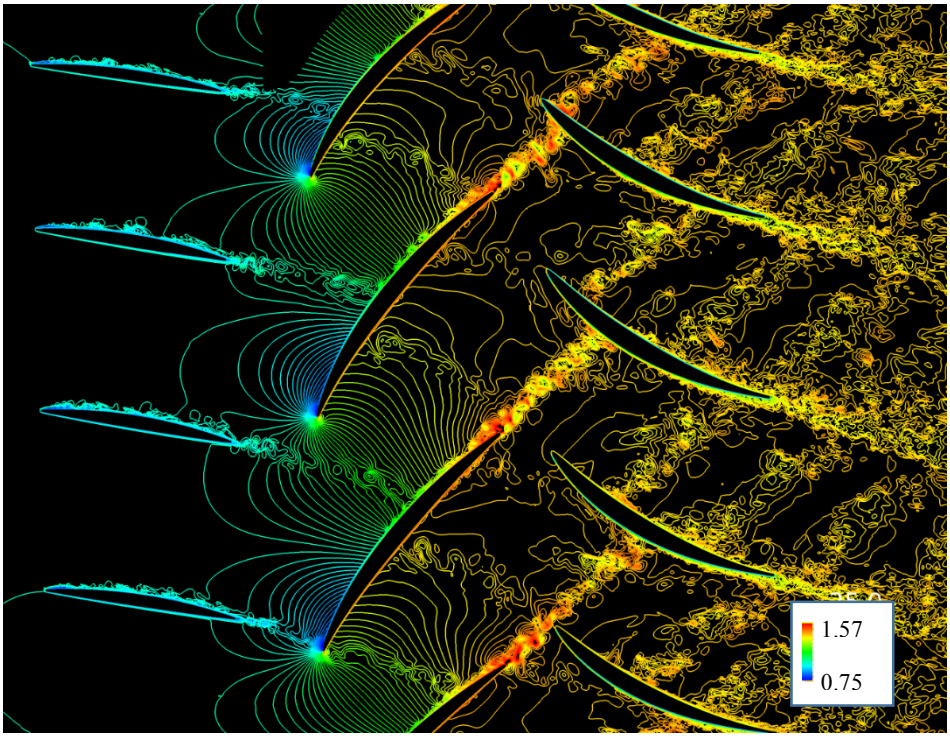

29% Spacing

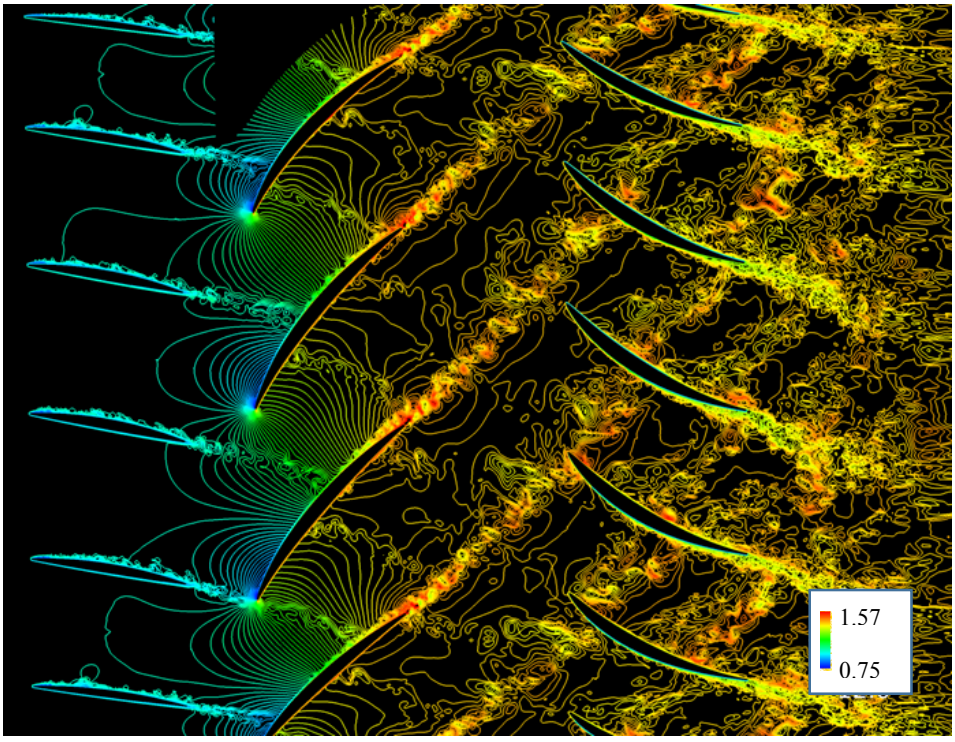

112% Spacing

Figure 4. Comparison of instantaneous total pressure distribution at 30% span

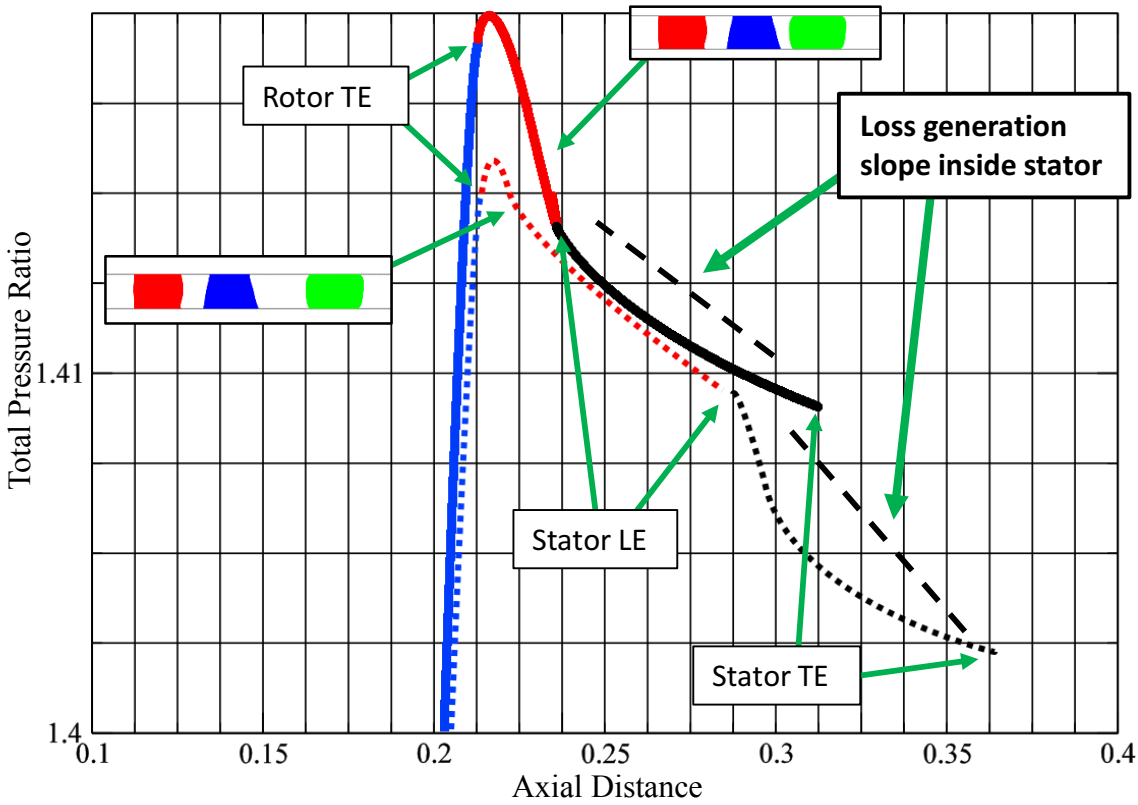

Figure 5. Absolute total pressure rise from rotor leading edge to stator trailing edge

dispersion with varying space between the rotor and the stator have been reported. Smith [1966] reported that compressor efficiency is increased about 1.2% when the axial spacing is reduced in a four-stage low speed axial compressor. Details of the loss development inside the stator as the rotor wake interacts with the stator blade and is stretched through the stator passage have not been fully explained. Experimental investigation of this phenomena requires direct measurements of the unsteady velocity and transient pressure field inside the stator passage with great accuracy. At the moment, no such experimental investigations are planned, even though the wake dispersion/recovery is one of the essential mechanisms of multi-stage compressor physics. Therefore, the current numerical study based on a LES is undertaken.

The total pressure recovery from wake stretching is the process of energy transfer from turbulence to the mean flow. Turbulence models in the conventional RANS and URANS do not simulate this reverse process of energy transfer. Therefore, a LES was applied for the present investigation. With spatially-filtered Navier-Stokes equations, the subgrid-scale stress tensor term needs to be modeled properly for the closure of the governing equations. A Smagorinsky-type eddy-viscosity model was used for the subgrid stress tensor, and the standard dynamic model by Germano et al. [1991] was applied.

In the current study, the governing equations are solved with a pressure-based implicit method using a fully conservative control volume approach. A third-order accurate interpolation scheme is used for the discretization of convection terms and central differencing is used for the diffusion terms. For the time-dependent terms, an implicit second-order scheme is used and a number of sub-iterations are performed at each time step. Approximately 8000 time steps are used for one rotor revolution.

Standard boundary conditions for the multi-blade rows were applied at the boundaries of the computational domain (Hah and Shin [2012]). The inflow boundary of the computational domain was

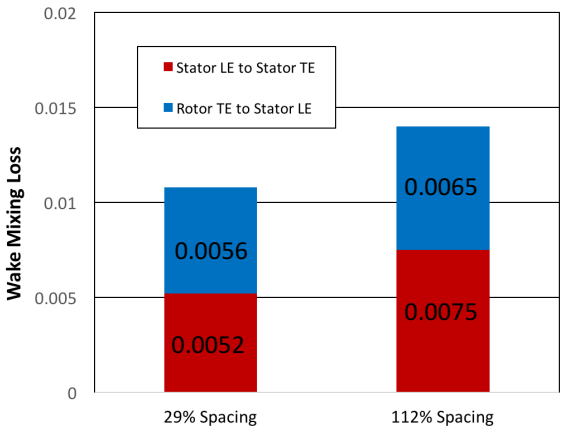

Figure 6. Breakdown of the wake mixing loss from rotor trailing edge to stator trailing edge

located 20 average blade heights upstream of the rotor leading edge in order to dampen out any possible reflections. Likewise, the outflow boundary was located 20 blade heights downstream from the trailing edge. Circumferentially averaged static pressure at the exit boundary casing was specified to control the mass flow rate. Non-reflecting boundary conditions were applied at the inlet and exit boundaries.

The current compressor stage has 20 IGV blades, 15 rotor blades, and 20 stator blades. One fifth of the compressor passage with the blade count of 4-3-4 was simulated. Several simulation grids were examined to see how well the wake recovery process is calculated, ranging from 500, 700, and 990 million total grid points for the 4-3-4 blades. Wake recovery was fairly well calculated with both the 700 and 990 million node grids. The final computational grid was 442 nodes for IGV, rotor and stator in the blade-to-blade direction, 384 nodes in the spanwise direction, and 402 nodes for IGV and rotor, 760 nodes for stator in the streamwise direction. The total number of 990 million grid nodes is used for the LES simulation. The rotor tip clearance geometry is represented by 90 nodes inside the tip gap in an attempt to accurately resolve the tip clearance flow field. I-grid topology is used to reduce grid skewness and a single-block grid is used. The wall resolution is within the range $Dx^+ < 10$, $Dy^+ < 2.0$, and $Dz^+ < 10$ in streamwise, pitchwise, and spanwise directions.

All the computations were performed with NASA's Pleiades supercomputing system, which allows parallel computation with multiple processors.

OVERALL FLOW FIELD AND TOTAL PRESSURE LOSS WITH DIFFERENT SPACING BETWEEN ROTOR AND STATOR

Instantaneous distributions of absolute total pressure at 30% span are compared in Figure 4. Instantaneous total pressure distributions in Figure 4 show that the rotor wake is stretched as it passes through the stator passage. The total pressure contours near the stator blade in Figure 4 show the effects of rotor wake interaction with the stator blade boundary layer are quite different between the suction side and the pressure side of the stator blade. Figure 4 shows that the IGV wake is not fully decayed at the rotor exit and it passes through the stator together with the rotor wake. As shown in Figure 4, the unsteady flow field in the stator passage is very complex. Three main mechanisms of the total pressure change in the stator passage are wake recovery due to the wake stretching, viscous mixing of the wake, and the unsteady stator boundary layer development from the rotor wake interaction. A previous study by Van Zante et al [2002] concluded that total pressure loss due to the viscous wake mixing is very small compared to the two other effects.

To examine steady total pressure loss through the stator passage, calculated instantaneous flow fields were averaged over one rotor revolution. Figure 5 shows the mass-averaged absolute total pressure rise from the rotor leading edge to the stator tailing edge for two stage configurations. Overall total pressure rise is about 0.5% higher for the close spacing (29% spacing, case A) than the wider spacing (112% spacing, case B). About 63% of the total pressure gain by the reduced gap between the rotor and the stator is due to the difference in upstream effects of the stator pressure field. 15% of total pressure difference is from the reduced mixing loss from the rotor exit to the leading edge of the stator. The remaining 22% of the total pressure gain comes from the difference in the wake recovery in the stator passage. The

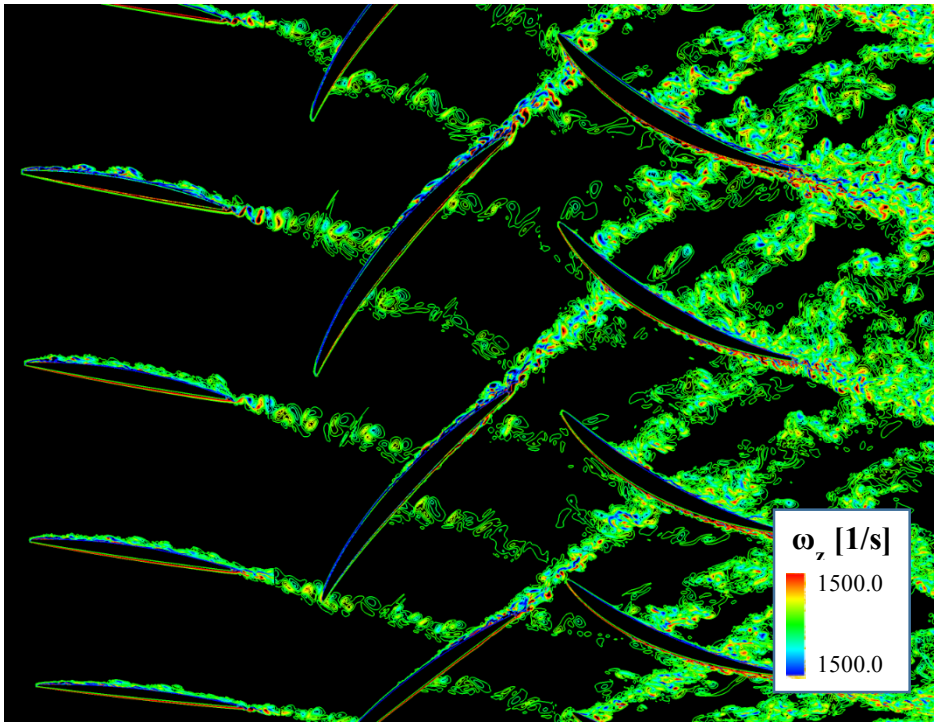

Figure 7. Instantaneous distribution of radial vorticity component at 30% span with 29% spacing

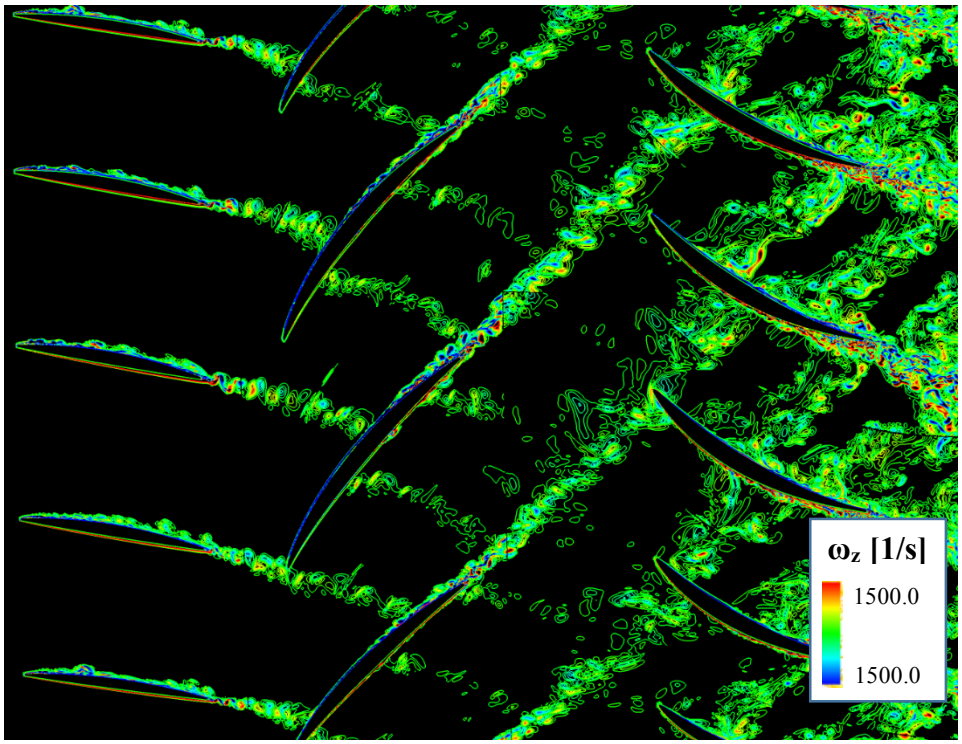

Figure 8. Instantaneous distribution of radial vorticity component at 30% span with 112% spacing

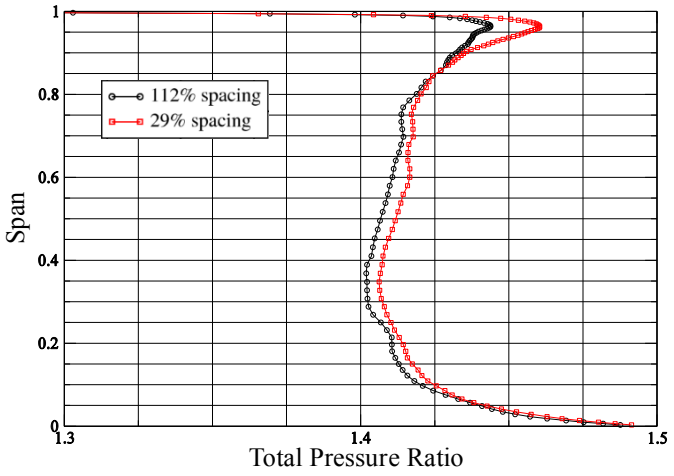

Figure 9. Total pressure distribution at rotor exit

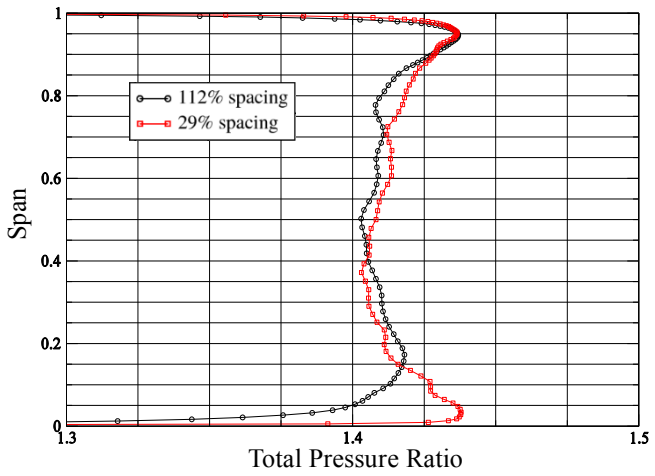

Figure 10. Total pressure distribution at stator leading edge.

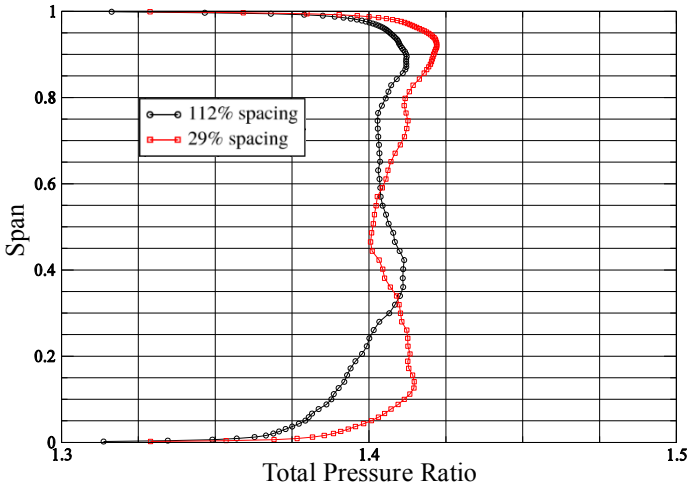

Figure 11. Total pressure distribution at stator trailing edge.

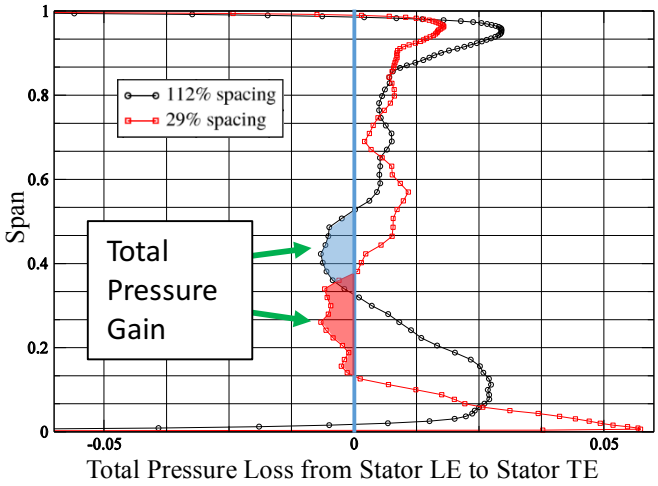

Figure 12. Change in total pressure from stator leading edge to stator trailing edge

difference in loss generation from the stator leading edge to the stator trailing edge between the two cases is indicated clearly by the slopes in Figure 5. The reduced loss generation inside the stator passage with the smaller axial gap is due to the difference in wake recovery. The breakdown of wake mixing loss from the rotor trailing edge to stator trailing edge is shown in Figure 6. The overall wake mixing loss in the stator is reduced by about 25% by narrowing the gap between the rotor and the stator from 112% to 29%. Figures 7 and 8 compare the instantaneous radial vorticity component in the rotor wake at 30% span. The vorticity is much stronger with the smaller axial gap at the entrance of the stator. The rotor wake entering the stator has a sharper shape with more unsteady energy, which results in higher total pressure recovery with the wake stretching as it passes through the stator passage. The current one and one half stage compressor has a low aspect ratio, as shown in Figure 2, and the overall efficiency gain through the wake recovery is expected to be lower than compressors with high aspect ratios. The calculated total pressure gain by reduced axial spacing between the rotor and the stator is in the

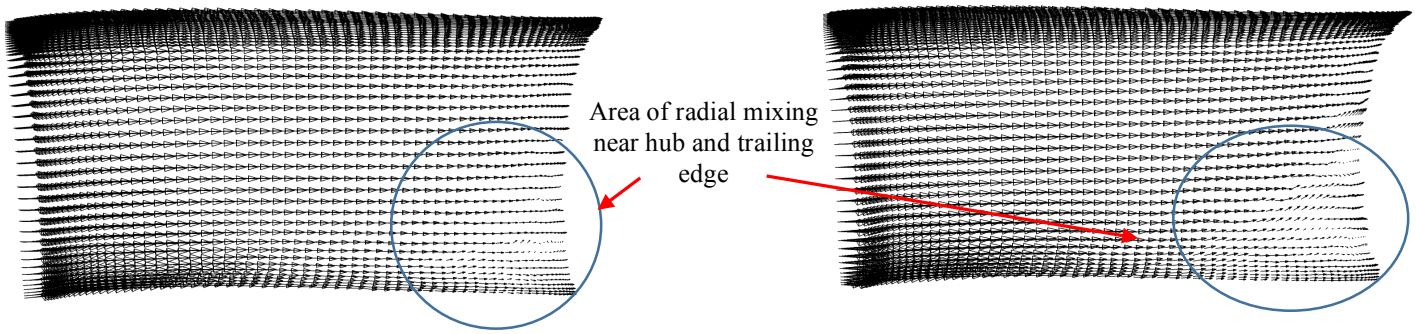

29% Spacing

112% Spacing

Figure 13. Time-averaged velocity vectors at 2.5 % pitch away from the suction side of the stator at trailing edge.

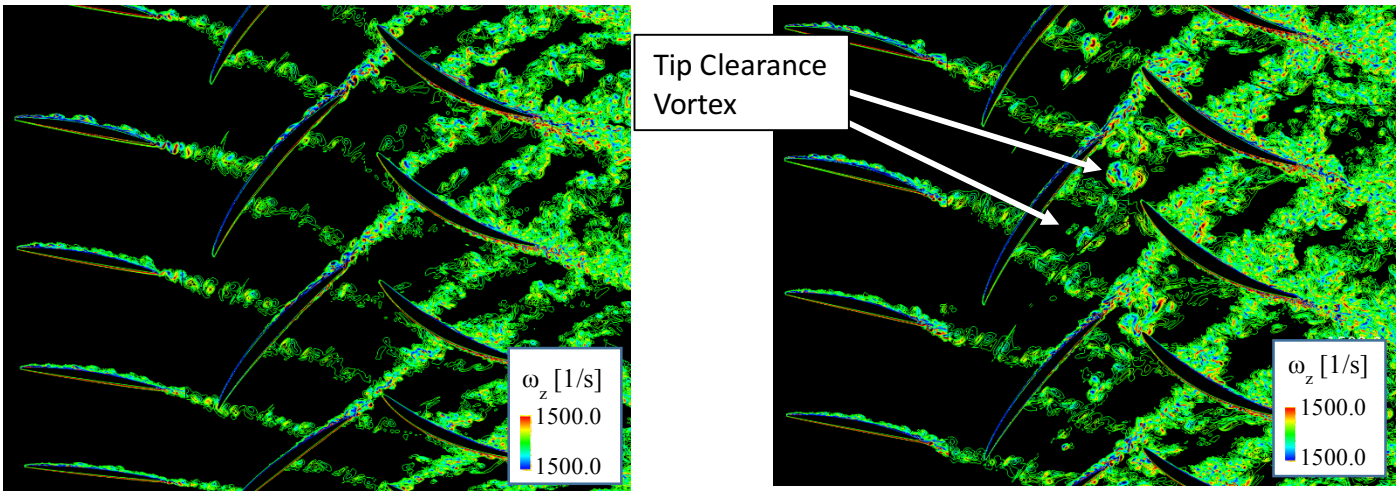

30% Span

50% Span

Figure 14. Comparison of instantaneous radial vorticity at 30% and 50% span with 29% axial spacing

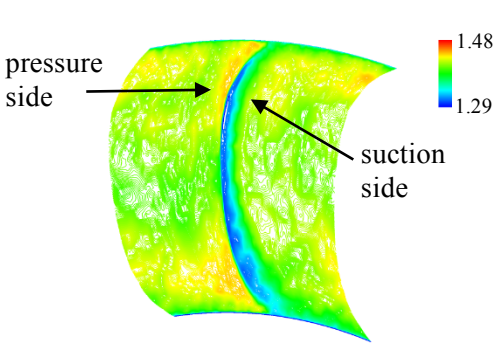

Figure 15. Time-averaged total pressure distribution at stator trailing edge, 29% spacing

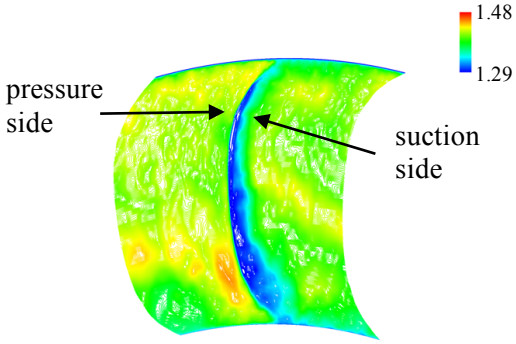

Figure 16. Time-averaged total pressure distribution at stator trailing edge, 112% spacing.

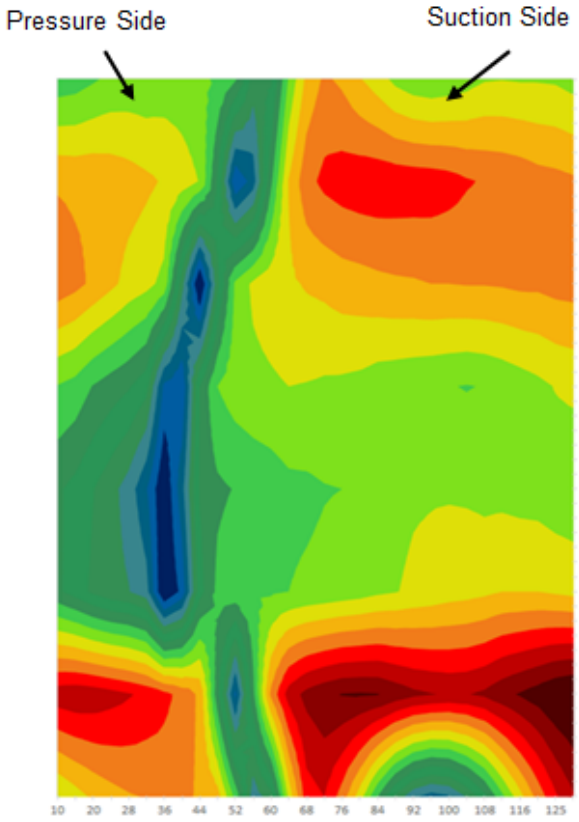

Figure 17. Measured total pressure distribution at stator exit in a one and one half stage high speed compressor (Lurie and Breeze-Stringfellow [2015])

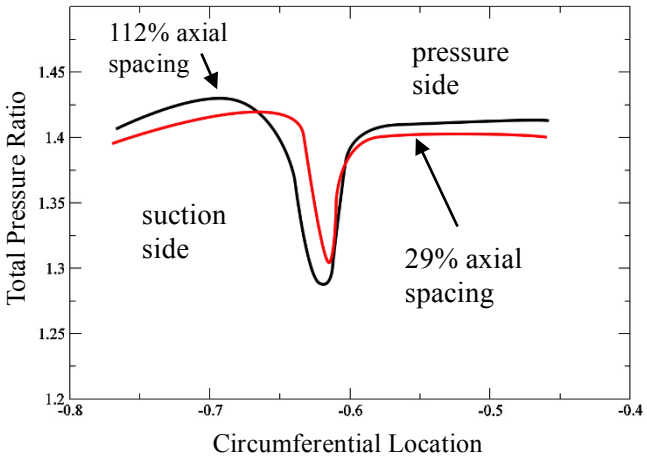

Figure 18. Comparison of tangential distribution of total pressure at 50% span

similar range of previously explained values (Smith [1996]).

RADIAL VARIATION OF TOTAL PRESSURE LOSS

Radial distributions of mass averaged total pressure at the rotor exit, stator inlet, and stator exit are compared in Figures 9, 10, and 11 for the two axial gaps. In Figures 9, 10, and 11, the total pressure is normalized with the rotor inlet total pressure. Between the rotor exit and the stator inlet, the radial distribution of the total pressure remains very similar above 20% span. A significant boundary layer develops near the hub between the rotor trailing edge and the stator leading edge. With 112% spacing, more boundary layer develops with a longer wetted endwall area as shown in Figure 10. At the inlet of the stator, total pressure is higher near the hub and the casing. Changes in total pressure from the stator inlet to the stator exit are compared in Figure 12 for the two axial gaps. As shown in Figure 12, total pressure is actually increasing from 17% span to 36% span for the close gap, and 33% span to 53% span for the wider gap. The increase in total pressure through the stator passage in these radial sections could come from the wake recovery and/or radial mixing of high total pressure fluid near the hub section. Time-averaged velocity vectors at 2.5% pitch away from the suction surface near the trailing edge of the stator are shown in Figure 13. Most radial flow in the stator passage occurs near the suctions side for the current stator passage. As shown in Figure 13, radial flow becomes much smaller away from the blade. As the radial transport of the fluid with high total pressure near the hub occurs over the very small area near the blade for the present compressor, radial redistribution of total pressure by the radial mixing is considered small.

As shown in Figures 5 and 6, the total pressure loss is reduced about 5% when the axial gap is reduced from 112% to 29% of the axial chord at mid-span. The reduction of loss generation with the reduced axial gap is due to the difference in wake recovery. Figure 12 shows that the largest difference in total pressure loss in the stator between the two spacings occurs between 10–35 % span. Instantaneous contours of total pressure and

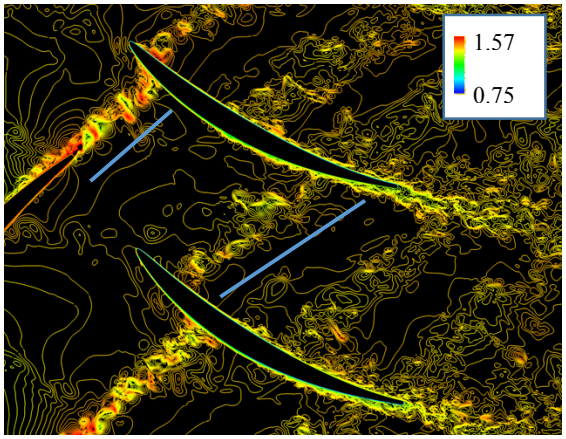

Figure 19. Instantaneous distribution of total pressure at 30% span with 29% axial spacing

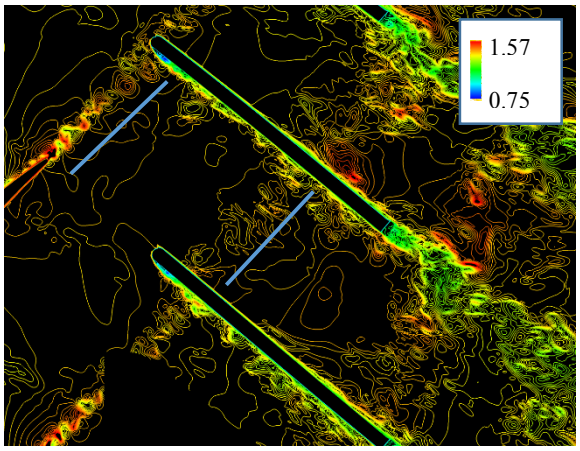

Figure 20. Instantaneous distribution of total pressure at 30% span, 29% spacing with flat plate stator

the radial vorticity at 30% span shown in Figures 4, 7, and 8 indicate that the flow at this span does not show any significant effects of radial mixing. At 30% span, instantaneous flow structures clearly show the stronger rotor wake is entering the stator passage with 29% spacing, which results in more wake recovery.

Instantaneous distribution of the radial vorticity component at 30% and 50% of the span with the 29% axial gap are compared in Figure 14. At 50% span, some vortices from the tip clearance flow appear near the rotor's trailing edge. These vortices from the tip clearance flow make the rotor wake thicker as it enters the stator passage. As shown in Figure 14, the rotor wake is sharper at 30% span than at 50% span. The sharper wake shape going into the stator passage leads to higher wake recovery.

Increased loss area near pressure side of the stator blade at mid-span

Figures 15 and 16 compare time-averaged total pressure distribution at the stator exit. For both axial gaps, the total pressure is lower near mid-span and a region with high total pressure loss is created near the pressure side of the stator blade at mid-span. A recent experimental study to investigate unexpectedly high loss generation in a high-speed compressor by Lurie and Breeze-Stringfellow [2015] also reported an area with high total pressure loss near the pressure side of the stator, as shown in Figure 17. The time-averaged total pressure distribution at the stator exit in the current low-speed compressor, shown in Figures 15 and 16, is remarkably similar to that of the high-speed compressor in Figure 17. Pitchwise distributions of total pressure at mid-span are compared in Figure 18. Again, both compressor stages show a region with high total pressure loss near the pressure side of the blade at mid-span. The boundary layer on the suction surface becomes much thicker as the axial spacing increases from 29% to 112%, as shown in Figure 18. The contour plots in Figures 15 and 16 show that the suction surface boundary layer development becomes much smaller as the axial spacing is reduced, especially below mid-span. Larger wake recovery near the suction surface with the narrower axial spacing is the main reason for this difference in blade boundary layer development.

The time-averaged total pressure distribution, which is measured by steady probes, is the average of rotor wake and the free stream passing through the stator exit. Instantaneous distribution of total pressure in the stator passage at 30% span with the 29% axial gap is shown in Figure 19.

Turbulence generation is expressed in the following equation with a local coordinate system (Soranna et al. [2006]):

$$P_{ij} = -\overline{u_i' u_k'} \frac{\partial \overline{U_j}}{\partial x_k} - \overline{u_j' u_k'} \frac{\partial \overline{U_i}}{\partial x_k}$$

In non-equilibrium turbulence, generation and dissipation of turbulence is not the same. Turbulence energy can be transferred from the small scale turbulence to the mean flow with a larger length scale. Turbulent flow near the stagnation point at the blade leading edge is an example. The detailed energy transfer mechanism in a compressor blade row was explained by Soranna et al. [2006]. When the rotor wake is stretched in the stator passage, the strain rate and the turbulence generation both become negative, which means there is energy transfer from the turbulence to the mean flow. The strain rate is much greater near the suction side than near the pressure side. At 5% axial chord into the stator passage, the strain rate near the suction side is more than two times larger than that near the pressure side as fluid in the wake near the suction surface moves much faster along the suction side of the blade. With the larger negative strain rate near the suction side, more total pressure recovery occurs near the suction surface than near the pressure surface.

Also, concave longitudinal curvature on the pressure side increases viscous mixing (increased loss) near the pressure side (Prandtl [1929]). Intra-transport of rotor wake inside the stator passage explained by Kerrbrock and Mikolajcak [1970] is very small for the current compressor as the slip velocity inside the stator passage becomes negligible when the wake enters the stator passage (Hah [2015]). Therefore, the loss core near the pressure side of the stator blade is generated by smaller wake recovery compared to that near the suction surface and added mixing loss due to the curvature effect. To examine the overall effect of blade curvature and wake stretching numerically, a LES was performed with a flat plate stator. Instantaneous total pressure distribution with the flat plate stator is given in Figure 20. With the flat plate stator, there is very little wake stretching and no wake recovery. Since there is no blade curvature with the flat plate, total pressure distribution is almost the same on the pressure side and the suction side. The Asymmetric total pressure distribution with the high loss region near the pressure side at the stator exit shown in Figures 15 and 16 is due to the larger wake recovery near the suction side and the larger viscous mixing near the pressure side due to the convex curvature of the pressure side of the blade. The generation of the low total pressure area near the pressure side at mid-span observed in a high speed compressor stage (Lurie and Breeze-Stringfellow [2015]) is due to the same mechanism shown in the current low speed compressor stage.

CONCLUDING REMARKS

Effects of rotor wake dispersion in the stator of a low-speed one and one half stage axial compressor are investigated in detail. Numerically simulated flow fields with LES are examined in detail to quantify wake recovery due to inviscid wake stretching and loss generation from the interaction between the rotor wake and the stator blade boundary layer. The following are the major conclusions:

1. The compressor's total pressure loss is decreased 0.5% by reducing the axial gap between the rotor and the stator in the current one and one half stage axial compressor. The LES shows that about 22% of the efficiency gain is due to the wake recovery and about 63% is due to the unsteady non-uniform pressure field at the rotor exit, which is generated by the upstream influence of the stator's pressure field.
2. Due to the rotor tip clearance and the end wall boundary layers, the absolute total pressure entering the stator is higher both near the hub and near the casing. The wake recovery is much higher near the hub for the current compressor stage. The total pressure recovery by the wake stretching is larger than the total pressure loss due to the interaction between the rotor wake and

the stator blade boundary layer over a small radial section around 30% span for both axial gaps. This is due to a stronger rotor wake entering the stator passage in this section and the resulting larger wake recovery. The rotor tip clearance flow affects the flow field down to mid-span for the current compressor. As the tip clearance flow moves radially inward, the rotor wake becomes thicker before entering the stator, resulting in less wake recovery. This effect of tip clearance flow should be considered when the wake recovery effect is considered for the compressor stage design.

3. High loss areas near the pressure side at mid-span are observed at the stator exit plane. This high loss area near the pressure side of the blade is created by two flow mechanisms. First, total pressure recovery by the wake stretching near the pressure side is much smaller than that near the suction side of the blade. Second, the longitudinal curvature effect on the pressure side creates more viscous mixing and increased loss. A simple numerical experiment with flat plate stators shows that there is no wake stretching and no curvature effects, which results in nearly symmetric distribution of total pressure at the stator exit.

ACKNOWLEDGMENTS

The author gratefully acknowledges the support of this work by the NASA Fixed Wing AATT program. The author thanks Michael Romeo of Kent State University for assistance in generating the mesh and preparation of the final paper.

REFERENCES

Adamczyk, J.J., 1996, "Wake Mixing in Axial Flow Compressors," ASME Paper No.96-GT-029.

Ding, K., 1982, "Flow Measurements Using a Laser-Two-Focus Anemometer in a High-Speed Centrifugal and a Multistage Axial Compressor," presented at ASME Winter Annual Meeting, Phoenix, AZ.

Deregel, P. and Tan C.S., 1996, "Impact of Rotor Wakes on Steady-State Axial Compressor Performance," ASME Paper No. 96-GT-253.

Dunker R.J., 1983, "Flow Measurements in the Stator Row of a Single-Stage Transonic Axial-Flow Compressor with Controlled Diffusion Stator Blades," AGARD CP-351.

Germano, M., Piomelli, U., Moin, P., and Cabot, W. H., 1991, "A Dynamic Subgrid-Scale Eddy-Viscosity Model," Journal of Fluid Mechanics, Vol. A3, pp. 170-176.

Gourdain, N., 2013, "Validation of Large Eddy Simulation for the Prediction of Compressible Flow in an Axial Compressor Stage," ASME paper GT 2013-94550.

Hah, C., 2015, "Effects of Unsteady Flow Interactions on the Performance of a Highly-Loaded Transonic Compressor Stage," ASME Paper, GT2015-43389.

Hah, C. and Shin, H., 2012, "Study of Near –Stall Flow Behavior in a Modern Transonic Fan with Compound Sweep," ASME Journal of Fluids Engineering, Vol.134, pp.071101-071107.

Hah C. and Katz J., 2014 "Investigation of Tip Leakage Flow in an Axial Water Jet Pump with Large Eddy Simulation," proceedings of 30th Naval Hydrodynamics Symposium, Hobart, Australia.

Hah, C., Hathaway, M., and Katz, J., 2014, "Investigation of Unsteady Flow Field in a Low Speed One and a Half Stage Axial Compressor: Effects of Tip Gap Size on the Tip Clearance Flow Structure at Near Stall Operation," ASME paper GT2014-27094.

Hah, C., 2016, "Effects of Double-Leakage Tip Clearance Flow on the Performance of a Compressor Stage with a Large Rotor Tip Gap," ASME Paper GT2016-56056.

Hathaway, M.D., 1986, "Unsteady Flows in a Single-Stage Transonic Axial-Flow Fan Stator Row," NASA TM 88929.

Kerrebrock J.L. and Mikolajczak A. A., 1970, “Intra-Stator Transport of Rotor Wakes and Its Effect on Compressor Performance,” ASME Journal of Engineering for Power, Vol.92, pp 359-368.
Lurie, D.P. and Breeze-Stringfellow, A, 2015, “Evaluation of Experimental Data from a Highly Loaded Transonic Compressor Stage to Determine Loss Sources,” ASME Paper GT2015-42526.
Papadogiannis, D., Duchane, F., Sicot, F., Gicquel, L., Wang, G., and Moreau, S, 2014, “Large Eddy Simulation of High Pressure Turbine Stage: Effects of Sub-Grid Scale Modeling and Mesh Resolution,” ASME paper GT2014-25876.
Pallot, G., Kato, D., Kanameda, W., and Ohta Y., 2016, “Effect of Incoming Wakes on the Stator Performance in a Single-Stage Low Speed Axial Flow Compressor Operating at Design and Near Stall Conditions,” ASME Paper GT2016-57981.
Prandtl, L., 1929, "Effect of stabilizing forces of turbulence," NACA TM 625.
Smith L. H. Jr., 1966, “Wake Dispersion in Turbomachines,” ASME Journal of Basic Engineering, Vol. 88.
Smith L. H. Jr., 1970, “Casing Boundary Layers in Multistage Axial-Flow Compressors,” Flow Research in Blading, edited by L.S. Dzung, Elservier Publishing Company, Amsterdam, 1970.
Smith L. H. Jr., 1996, “Discussion of ASME Paper No. 96-GT-029: Wake Mixing in Axial Flow Compressors,” ASME Turbo Expo, Birmingham, England.
Soranna, F., Chow, Y., Uzol, O., and Katz, J., 2006, “The Effects of Inlet Guide Vanes Wake Impingement on the Flow Structure and Turbulence around a Rotor Blade,” ASME Journal of Turbomachinery, Vol. 128, pp 82-95.
Valkov, T.V., 1997, “The Effect of Upstream Vortical Disturbances on the Time-Averaged Performance of Axial Compressor Stators,” Ph.D. dissertation, Massachusetts Institute of Technology.
Van Zante, D.E., Adamczyk, J.J., Strazisar, A.J., Okiishi, T.H., 2002, “Wake Recovery Performance Benefit in a High Speed Axial Compressor,” ASME Journal of Turbomachinery, Vol.124, pp 275-284.
Wasserbauer, C. A., Weaver, H. F., and Senyitko, R. G., “NASA Low-Speed Axial Compressor for Fundamental Research, “NASA TM 4635, Feb. 1995.
Williams, M.C., 1988, “Inter and Intrablade Row Laser Velocimetry Studies of Gas Turbine Compressor Flows,” ASME Journal of Turbomachinery, 110, pp 369-376.
Zaki, T, Wissink, J., Durbin, P.A., and Rodi, W., 2010, “Direct Numerical Simulations of Transition in a Compressor Cascade: the Influence of Free-Stream Turbulence,” J. of Fluid Mechanics, Vol. 665, pp 57- 98.